Advances in Geosciences Konstantinos Perakis & Athanasios Moysiadis, Editors
EARSeL, 2012

Potential of Airborne Laser Scanning Data for Classification of Wadden Sea Areas

Alena Schmidt[1], Winny Adolph[2], Sascha Klonus[3], Manfred Ehlers[3], Hubert Farke[2] and Uwe Soergel[1]
[1] *Leibniz University Hannover, Institute of Photogrammetry and GeoInformation, Hannover, Germany; {alena.schmidt, soergel}@ipi.uni-hannover.de*
[2] *Wadden Sea National Park of Lower Saxony, Wilhelmshaven, Germany; Winny.Adolph@nlpv-wattenmeer.niedersachsen.de*
[3] *University of Osnabrueck, Institute for Geoinformatics and Remote Sensing, Osnabrueck, Germany; {sklonus, mehlers}@igf.uni-osnabrueck.de*

Abstract. The classification and mapping of habitats in Wadden Sea areas is an important issue of marine monitoring. In the framework of a German research project, we investigate different modern remote sensing data for this task. In this paper, our focus is on the potential of airborne laser scanning data for the classification. Therefore, we use Conditional Random Fields (CRF), a probabilistic supervised classification approach capable of modelling context. We classify the laser scanning point cloud into the three object classes *water*, *mudflat*, and *mussel bed*. For the distinction of different surface types we analyse crucial classification features based on the geometry and the intensity of the backscatter. We then learn typical structures in a training step and combine local descriptors with context information in a CRF framework. We evaluate our approach on a test site of the German part of the Wadden Sea and show classification results of multispectral and SAR data which we intend to combine for a marine monitoring concept.

Keywords. LiDAR, classification, coast, water, conditional random fields.

1. Introduction

The Wadden Sea is a unique habitat in the southeastern part of the North Sea. Due to its biological diversity, in 2009, the German and the Dutch part of the Wadden Sea were inscribed on UNESCO's World Heritage List. However, it is influenced by climate change and human activities. For these reasons a recurrent monitoring of these areas becomes necessary. Therefore, new approaches for a sustainable monitoring are investigated in a German research project called Scientific Monitoring Concepts for the German Bight [1]. In this framework, we investigate the habitat mapping and classification of Wadden Sea areas in regard to a deeper understanding of the habitat composition. For the eulittoral zone, which is covered with seawater during high tide, but falls dry during low tide, the different habitats can be classified from remote sensing data. Thereby, we use three types of remote sensing data: SAR data, optical images, and airborne laser scanning data, also called LiDAR (Light Detection and Ranging). We classify data separately so far, but we aim at a combined classification approach. In this paper, our focus is on the classification of LiDAR data, which is necessary for two reasons.

Firstly, tidal flows, storms, climate change, and human activities cause morphological changes of various kinds. The morphology of the terrain can be represented by digital terrain models (DTM). The acquisition of highly accurate height data by laser scanning, however, is limited to the water surface because the near-infrared laser pulses cannot penetrate water. The generation of a DTM thus requires the detection of water surfaces within tidal channels, where residual water can remain even

during low tide. An additional data source, e.g. sonar, can be used to complete the DTM in these areas. This leads to the first crucial classification of LiDAR data into *land* and *water* areas.

Secondly, we are interested in the contribution of LiDAR data for the habitat mapping. This involves a separation of the class *land* into different subclasses. This has been shown to be possible with spectral information from remote sensing image data [2]. For classification based on monochromatic LiDAR, the distinction between the habitats is a difficult task, due to the lack of spectral features. On the other hand, besides the purely geometric measurement of 3D coordinates, modern LiDAR systems record also the intensity of the backscatter, which can provide information about additional target characteristics like roughness. In regard to the properties of LiDAR, only habitats characterised by their surface roughness, e.g. *mussel beds*, can be expected to be distinguished. Thus, we differentiate two subclasses of *land*, namely *mudflat* and *mussel bed*.

Figure 1 shows a high-resolution orthoimage and the LiDAR point cloud of our test site, a typical scene in the German Wadden Sea. It contains several *mussel beds*, which are characterised by a dark colour in the orthoimage (e.g. in the middle of the scene) and high elevation in the point cloud. In some parts of the *water* areas, e.g. the big water-filled tideway from west to east, no backscatter is recorded due to specular reflection of the laser pulse. In these regions lots of gaps in the point cloud occur.

In this paper, we present a supervised classification approach for LiDAR data in Wadden Sea areas. We distinguish the three classes *water*, *mudflat*, and *mussel bed*. Those objects, their typical structures, and interrelations are integrated in the classification process. Therefore, we use a Conditional Random Fields (CRF) framework. We focus on the extraction of optimal features for the classification of Wadden Sea areas and on the implementation of a CRF framework for LiDAR point cloud.

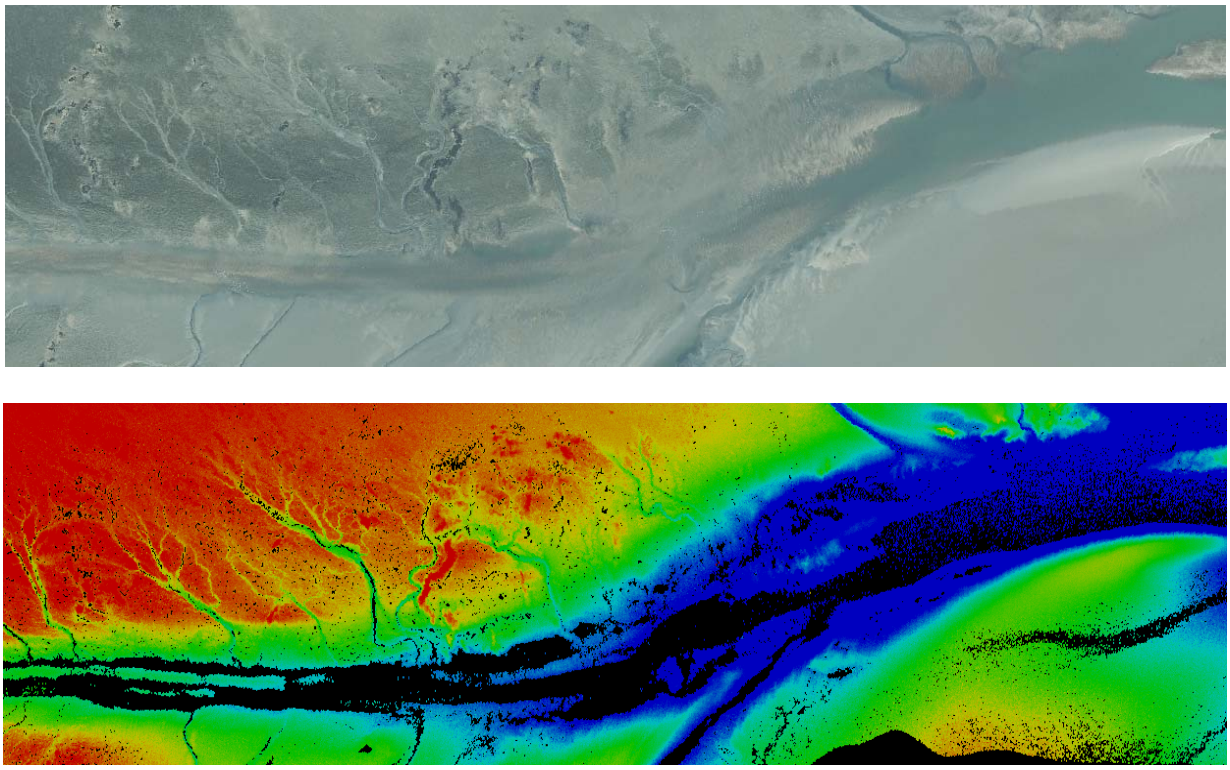

Figure 1: Orthoimage and point cloud (coloured by height from low (blue) to high (red)) of the test site in the German Wadden Sea. Because of specular reflection the number of laser pulses without any received return can be significantly higher in water surfaces (black).

2. Method

Our aim is to classify the LiDAR data by assigning a class label to each point in the point cloud. Because of the rather homogeneous appearance of the Wadden Sea, which mainly consists of flat areas with hardly any discriminative objects, the classification becomes challenging. Therefore, the classification task results in two crucial aspects. On the one hand, we need appropriate classification features for the distinction of different classes in this special test data. The feature extraction is investigated in Section 2.1. On the other hand, the CRF framework has to be implemented for the irregular point cloud. The structuring of the graph as well as the choice of parameters and functions for the training and inference are described in Section 2.2.

2.1. Feature extraction

For each laser pulse, information about 3D coordinates and intensity are available for the backscattered signal. We do not use full waveform laser scanner data and, thus, do not have additional signal waveform information. Nevertheless, several features can be calculated from the point cloud. We test different features based on the intensity, the average height and the curvatures and identify a representative set for our classification task by a correlation-based approach out of the WEKA data mining software [3]. Thus, eight features are indicated to be essential for the distinction of the classes *water*, *mudflat*, and *mussel bed*. The *intensity* and the *point density* have been found to be well-suited for separating *water* from dry *mud* areas in the Wadden Sea [4]. On water surfaces, the *intensity* may be low due to a lower reflectance (Figure 2). Because of specular reflection (dependent on the incidence angle), the number of laser pulses without any received return can be significantly higher in water surfaces, which leads to a decreasing *point density*.

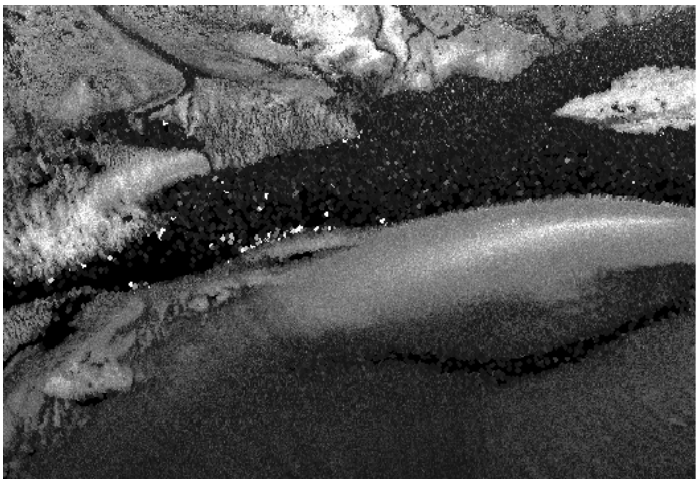

Figure 2: Intensity data of the backscattered signals which may be low (black) on water areas and high (white) on land surfaces.

For *mussel bed* detection, different features are derived from the local geometry of point distribution. Therefore, we use a volumetric approach and define a vertical cylinder with a predefined radius r to find adjacent points. The radii for the neighbourhood definition are set to $r_1 = 3\,m$ and $r_2 = 10\,m$, depending on the features. The difference of a point and the lowest point elevation value within the cylinder, depicted as *distance to ground*, characterises the greater elevation of this class. Further height-based features are the *average height* of all adjacent points in a neighbourhood as well as the *difference of average heights* for various radii. Moreover, we calculate the maximum and minimum of the normal curvature at a point on this plane, denoted as

principal curvatures k_1 and. The product of the principal curvatures is called the *Gaussian curvature*, the mean curvature $H = \frac{1}{2(k_1 + k_2)}$ can be determined by the mean arithmetic curvature. The deviation of points from a plane is derived from the three eigenvalues ($\lambda_1 \geq \lambda_2 \geq \lambda_3$) within the cylindrical neighbourhood based on the covariance matrix of the 3D coordinates set up for each point. The *lowest eigenvalue* λ_3 serves as classification feature. All the eight features are introduced in our classification approach.

2.2. Classification of LiDAR data using conditional random fields

CRFs are a flexible tool for classification tasks and belong to the group of graphical models. For image labelling, they were introduced in [5]. In comparison to image data, labelling of point clouds is even more challenging due to the irregular distribution of points in 3D space. Several approaches for the classification of point clouds based on CRFs have been developed in the past. For instance, [6] propose a method for the classification of terrestrial laser scanning data. The potential of CRFs for airborne laser scanning data was shown in [7] (segment-based) and in [8] (point-wise).

In the CRF framework, data are converted to a graphical model which considers the relations between data through a network of nodes and edges. The nodes are represented by the dataset, in our case, the points of the LiDAR point cloud. In order to preserve small objects, especially small *mussel bed* areas, we classify point-based without a preceding segmentation. Each node and point, respectively, is linked to its adjacent nodes by an edge. In contrast to common classification approaches, data points are not modelled to be conditionally independent. Thus, a class label C_i to each node *i* in the graph is assigned based on its feature vector $\boldsymbol{x}_i$ as well as on those obtained for all points in the defined neighbourhood N_i. The posterior distribution $P(C|\boldsymbol{x})$ of the class C given the observed data $\boldsymbol{x}$ is derived in a discriminative model. Following [3] the posterior distribution $P(C|\boldsymbol{x})$ can be written as:

$$P(C|\boldsymbol{x}) = \frac{1}{Z(\boldsymbol{x})} exp\left(\sum_{i \in S} A_i(\boldsymbol{x}, C_i) + \sum_{i \in S} \sum_{j \in N_i} I_{ij}(\boldsymbol{x}, C_i, C_j)\right), \qquad (1)$$

where the *partition function Z(**x**)* acts as normalization constant. It is needed for the transformation of potentials to probabilities. The energy term can be expressed as the sum of *association potentials* $A_i(\boldsymbol{x}, C_i)$ and *interaction potentials* $I_{ij}(\boldsymbol{x}, C_i, C_j)$ over the neighbourhood $\boldsymbol{N}$ and the data set $\boldsymbol{S}$. The *association potential* A_i indicates how likely a node *i* belongs to a class *C* given the observations $\boldsymbol{x}$ (Equation 2). The *interaction potential* I_{ij} is a function of all data $\boldsymbol{x}$ and measures how the classes of neighbouring points interact (Equation 3). Closely related to [3] we consider a log-linear formulation to model both potentials

$$A_i(\boldsymbol{x}, C_i = l) = exp(\boldsymbol{w}_l{}^T \boldsymbol{h}_i(\boldsymbol{x})), \qquad (2)$$

$$I_{ij}(\boldsymbol{x}, C_i = l, C_j = k) = \exp(v_{l,k}^T \ \mu_{ij}(\boldsymbol{x})). \qquad (3)$$

Vector $\boldsymbol{w}_l$ contains the weights of node features $\boldsymbol{h}_i(\boldsymbol{x})$ of each node *i*. In our case we use the features described in Section 2.2 which are normalised to unit one to get a robust inference. The feature vector $\mu_{ij}(\boldsymbol{x})$ is calculated for each point by the absolute difference of feature vectors for each point of neighbouring nodes i and j. The weight vector $v_{l,k}$ is learnt in a training process depending on the combination of classes l and k.

The best discrimination of the classes is obtained iteratively in an optimization framework by minimising a cost function which depends on both of the weight factors. The optimal label configuration is determined in an inference step. Thereby, $P(C|x)$ is maximized for given parameters based on an iterative message passing algorithm. For the training and inference, we apply the optimization method Limited Memory Broyden-Fletcher-Goldfarb-Shanno [9] and the Loopy Belief Propagation [10] as message passing algorithm, as implemented in M. Schmidt's Matlab Toolbox [11]. The result of training and inference is a probability value per class for each data point. The optimal label configuration based on maximising $P(C|x)$ is provided via maximum a posterior (MAP) probability estimate.

3. Results

We evaluate our classification approach with LiDAR data from the German Wadden Sea. The test site covers an area of about 0.3 km x 1.1 km in the south of the islands Spiekeroog and Langeoog (Figure 1). It contains a big water-filled tideway, some smaller tideways as well as *mussel bed.* Data were acquired at low tide during a Wadden Sea monitoring using a RIEGL LMS-Q560 LiDAR system. Information about 3D coordinates and intensity are available for the backscattered signal of each laser pulse. We compare the classification results to a reference that was generated by delineating *water* and *mussel bed* considering ground truth data and an orthoimage. For the necessary training step, we divided test data set into two parts. Thereby, the parameters are learnt on one half of a test site and tested on the other one.

Tables 1 and 2 show the classification results for completeness and correctness of the three classes. Since we are interested in the investigation of influence of contextual knowledge for the classification, we modify the value of the neighbourhood *N*. For *mudflat* areas, we achieve good results with more than 90% completeness and more than 98% correctness in both tests. The rates for correctness of *water* areas detection are not on the same level (between 66% and 71%). In particular the discrimination of *water* and *mudflat* leads to a certain rate of misclassification. Figure 3 shows a part of the test site where water filled tideway, is mostly correctly classified. However, the classification of *water* areas often fails in the transition zone between *water* and *mudflat* where elevation differences are low. The results of different neighbourhood demonstrate that the increased neighbourhood for the CRF approach helps increasing the results due to a strong smoothing. This effect is caused by the interaction potential, which is basically a smoothing term. For the *mussel bed* detection a low correctness and, in particular, completeness rate is obtained. The main reasons are that only few *mussel bed* regions are presented in the test site in comparison to the *mudflat* areas.

Table 1. Results for classification with neighbourhood N = 2.

	Mudflat	Water	Mussel bed
Completeness	98.5 %	51.6 %	46.8 %
Correctness	97.7 %	70.7 %	42.6%

Table 2. Results for classification with neighbourhood N = 4.

	Mudflat	Water	Mussel bed
Completeness	90.8 %	82.4 %	56.6 %
Correctness	98.8 %	66.3 %	8.5 %

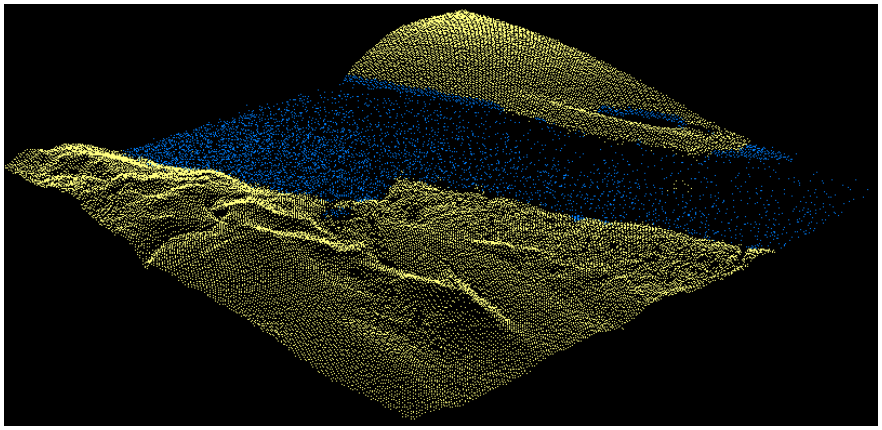

Figure 3: Labelled point cloud with *water* areas (blue) and *mudflat* areas (yellow).

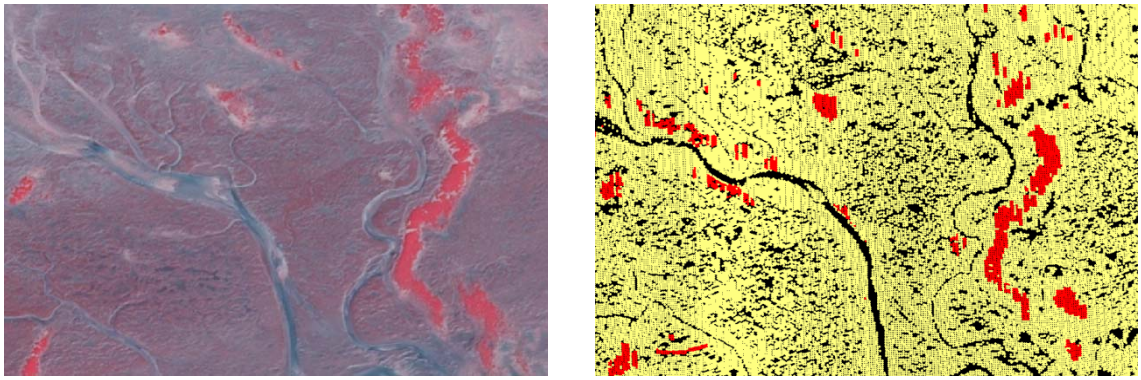

Figure 4: The Colour Infrared Orthoimage (left) of the test site clearly shows the mussel bed (red). In the labelled point cloud (right) most of them are detected (*mussel bed*: red, *mudflat*: yellow).

Therefore, the numbers of samples of available data for training and testing is limited. Moreover, *mussel bed* and *mudflat* are characterised by similar features in some parts of the test site. Most of the significant features for the *mussel bed* detection rely on the relative elevation differences as well as on the curvatures of the surface. These features occur very similar near to tideways and lead to misclassification in these parts (Figure 4). Nonetheless, the incorporation of context leads to partially high detection rates which can be seen in Figure 4, where the labelled point cloud is compared to the clearly recognisable *mussel bed* in the orthoimage.

4. Conclusions and Outlook

In this paper, a classification approach for remote sensing data in Wadden Sea areas has been described. In regard to a habitat mapping we use LiDAR data, SAR data, and optical images. The focus of this paper was on the classification method of LiDAR data. Therefore, we used a context-based approach in a CRF framework. We presented suitable classification features for a habitat mapping in Wadden Sea areas. As result of the supervised classification process, each point of the 3D point cloud is assigned to one of the three object classes *water*, *mudflat*, and *mussel bed*. A test on data of the German Wadden Sea showed that the detection of *water* and *mussel bed* in LiDAR data is a challenging task. For *water* areas, the best results were obtained for the contextual classification by increasing the neighbourhood, which leads to a stronger smoothing effect. In regard to the *mussel bed* detection, similar feature values, in particular based on relative height

differences and curvatures, leads to some misclassification of *mudflat* and *mussel bed* on the border of tideways.

In the future, we intend to integrate full waveform laser scanning data as well as some texture features in the classification process. Moreover, we plan to combine these data with classification results of optical images (Figure 5) and SAR images (Figure 6) to obtain a reliable concept for the marine monitoring. Visual interpretation of TerraSAR-X data in combination with profound ground-truth knowledge gained from extensive fieldworks or monitoring programmes allows the reliable identification of different surface structures like f. e. *mussel bed*, *mudflats* or *water* covered surfaces (Figure 6).

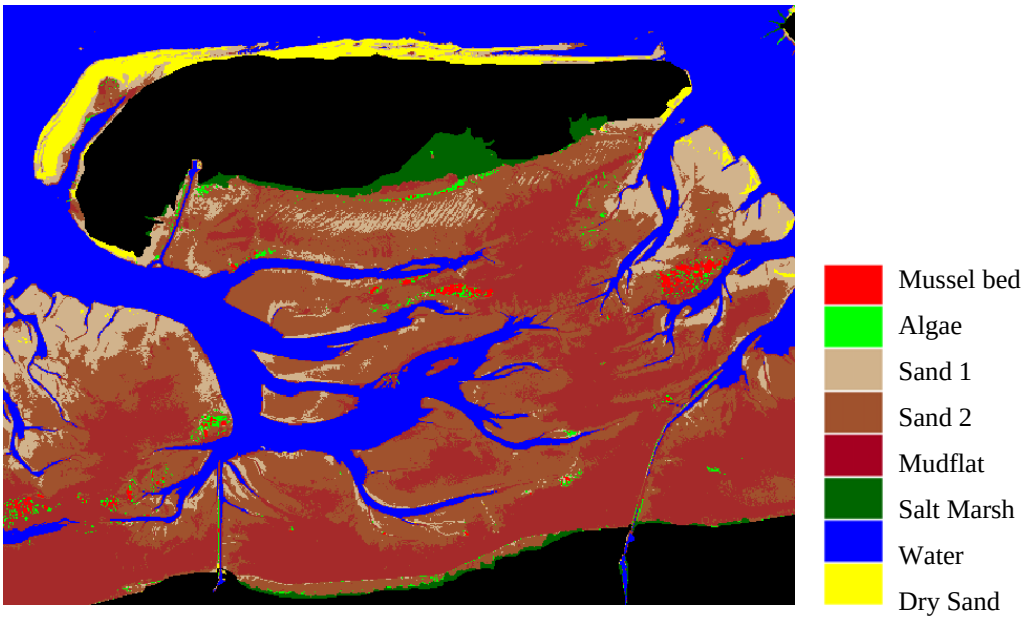

Figure 5: Classified RapidEye image.

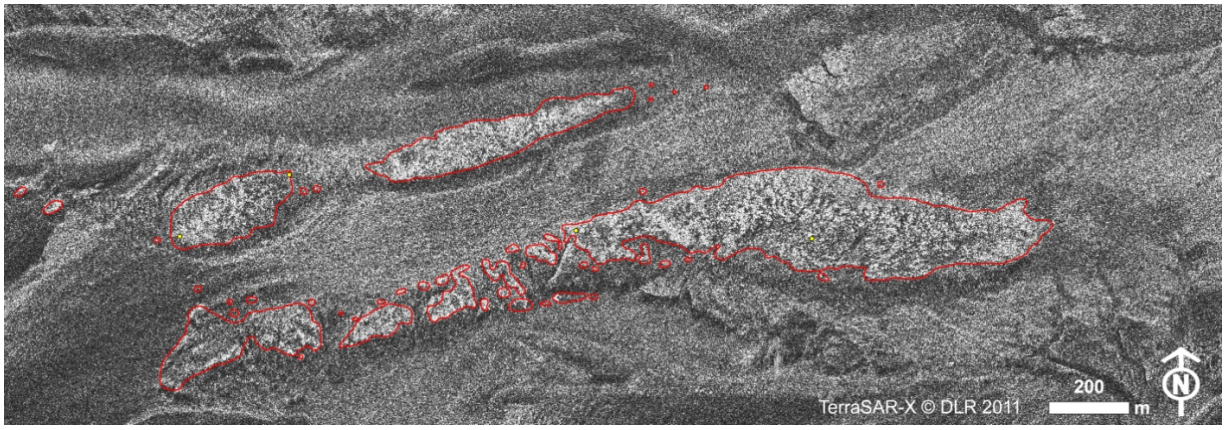

Figure 6: Detail from TerraSAR-X High Resolution Spotlight (©DLR, 2011) showing typical *mussel bed* structure verified by digital mapping from orthoimages (red contours) and ground-truth. The direct surroundings of the *mussel bed* are predominantly covered with *water* roughened by strong wind of 6 Beaufort. The image shows “Swinnplate” south of the island of Spiekeroog on 26.12.2011.

Acknowledgements

We would like to thank the Wadden Sea National Park of Lower Saxony for providing the orthoimages and ground truth data. We also thank the Lower Saxon State Department for Waterway, Coastal and Nature Conservation (NLWKN) for providing the LiDAR data.

References

[1] WIMO, 2012. Wissenschaftliches Monitoringkonzepte für die Deutsche Bucht, http://wimo-nordsee.de (May 4, 2012).

[2] Klonus, S., Tomowski, D., Ehlers, M., and Wohlfahrt, R., 2011. Potential of Rapideye image data for Wadden Sea monitoring. *Proceedings of 32nd EARSeL Symposium 2011*, Prague, CD, 9 pp.

[3] Witten, I. H. and Frank, E., 2005. *Data mining: practical machine learning tools and techniques*. 2nd edition. Morgan Kaufmann, San Francisco.

[4] Brzank, A., Heipke, C., Goepfert, J. and Soergel, U., 2008. Aspects of generating precise digital terrain models in the Wadden Sea from lidar - waterclassification and structure line extraction. *ISPRS Journal of Photogrammetry and Remote Sensing*, 63(5), pp. 510-528.

[5] Kumar, S. and Hebert, M., 2006. Discriminative Random Fields. *International Journal of Computer Vision*, 68(2), pp. 179–201.

[6] Lim, E. H. and Suter, D., 2009. 3d Terrestrial Lidar Classifications with Super-Voxels and Multi-Scale Conditional Random Fields. *Computer-Aided Design*, 41(10), pp. 701–710.

[7] Shapovalov, R., Velizhev, A. and Barinova, O., 2010. Non-associative Markov Networks for 3d Point Cloud Classification. In: *Proceedings of the ISPRS Commission III symposium - PCV 2010, International Archives of the Photogrammetry, Remote Sensing and Spatial Information Sciences, 38/Part A, ISPRS*, Saint-Mandé, France, pp. 103–108.

[8] Niemeyer, J., Wegner, J., Mallet, C., Rottensteiner, F. and Soergel, U., 2011. Conditional random fields for urban scene classification with full waveform lidar data. Photogrammetric Image Analysis (PIA), Lecture Notes in Computer Science, Vol. 6952, Springer Berlin / Heidelberg, pp. 233-244.

[9] Liu, D. C. and Nocedal, J., 1989. On the Limited Memory BFGS method for large scale optimization. *Mathematical Programming*, 45, pp. 503-528.

[10] Frey, B. and MacKay, 1998. *A revolution: Belief propagation in graphs with cycles. Advances in Neural Information Processing Systems* 10, pp. 479-485.

[11] Schmidt, M., 2012. UGM: A Matlab toolbox for probabilistic undirected graphical models, http://www.di.ens.fr/~mschmidt/Software/UGM.html (February 15, 2012).